Materials Science & Engineering C 131 (2021) 112518

Contents lists available at ScienceDirect

Materials Science & Engineering C

journal homepage: www.elsevier.com/locate/msec

Sonochemically engineered nano-enabled zinc oxide/amylase coatings prevent the occurrence of catheter-associated urinary tract infections

Aleksandra Ivanova [a], Kristina Ivanova [a], Ilana Perelshtein [b], Aharon Gedanken [b], Katerina Todorova [c], Rositsa Milcheva [c], Petar Dimitrov [c], Teodora Popova [d], Tzanko Tzanov [a,*]

[a] Group of Molecular and Industrial Biotechnology, Department of Chemical Engineering, Universitat Politècnica de Catalunya, Rambla Sant Nebridi 22, 08222, Terrassa, Spain
[b] The Department of Chemistry and Institute for Advanced Materials and Nanotechnology, Bar-Ilan University, Ramat-Gan 52900, Israel
[c] Institute of Experimental Morphology, Pathology and Anthropology with Museum, Bulgarian Academy of Sciences, Geo Milev, 1113 Sofia, Bulgaria
[d] Faculty of Veterinary Medicine, University of Forestry, 10 Sveti Kliment Ohridski Ave, 1756 Sofia, Bulgaria

ARTICLE INFO

Keywords:
Sonochemistry
Amylase
Zinc oxide nanoparticles
Biofilm inhibition
Bacterial infections prevention

ABSTRACT

Catheter-associated urinary tract infections (CAUTIs), caused by biofilms, are the most frequent health-care associated infections. Novel antibiofilm coatings are needed to increase the urinary catheters' life-span, decrease the prevalence of CAUTIs and reduce the development of antimicrobial resistance. Herein, antibacterial zinc oxide nanoparticles (ZnO NPs) were decorated with a biofilm matrix-degrading enzyme amylase (AM) and simultaneously deposited onto silicone urinary catheters in a one-step sonochemical process. The obtained nano-enabled coatings inhibited the biofilm formation of *Escherichia coli* and *Staphylococcus aureus* by 80% and 60%, respectively, for up to 7 days *in vitro* in a model of catheterized bladder with recirculation of artificial urine due to the complementary mode of antibacterial and antibiofilm action provided by the NPs and the enzyme. Over this period, the coatings did not induce toxicity to mammalian cell lines. *In vivo*, the nano-engineered ZnO@AM coated catheters demonstrated lower incidence of bacteriuria and prevent the early onset of CAUTIs in a rabbit model, compared to the animals treated with pristine silicone devices. The nano-functionalization of catheters with hybrid ZnO@AM coatings appears as a promising strategy for prevention and control of CAUTIs in the clinic.

1. Introduction

Indwelling medical devices such as urinary catheters have become an indispensable part of the modern medicine, aiding to improve the patient's quality of life [1]. However, all types of urinary catheters are vulnerable to microbial contamination and create an ideal environment for pathogenic bacteria to form biofilms originating severe urinary tract infections (UTIs) [2]. Catheter-associated UTIs (CAUTIs) account for over 40% of all hospital-acquired infections and more than 80% of all UTIs [3]. These infections are global health concern responsible for increased mortality and morbidity, prolonged time of hospitalization, elevated healthcare costs, lengthy antibiotic therapy and risk of resistance development [4].

Biofilm formation on urinary catheters is fundamental to CAUTIs pathogenesis [5]. Bacterial biofilms are complex structures of surface attached cells, which are embedded within a self-produced extracellular polymer matrix (EPM). Biofilm EPM is comprised mainly of polysaccharides, proteins and nucleic acids originating from both bacteria and the surrounding environment [6]. Among those, matrix exopolysaccharides (EPS) are integral part of the biofilm structure that assist bacteria to strongly adhere to the catheter surfaces and provide protection against antibiotic treatments. As a result, bacteria within biofilms effectively circumvent the existing antibiotic therapies and host immune defenses, causing difficult-to-treat infections, systemic dissemination of the pathogen and dysfunction of the medical device [7].

Current practices to decrease the incidence of CAUTIs consist in the frequent replacement of the contaminated device and aggressive antibiotic treatment, causing patients' discomfort and selection for new antimicrobial resistant (AMR) bacteria, respectively. Replacement of the contaminated catheter is only a temporary solution, as the newly inserted device provides a fresh surface for bacteria to readily adhere

* Corresponding author.
E-mail address: tzanko.tzanov@upc.edu (T. Tzanov).

https://doi.org/10.1016/j.msec.2021.112518
Received 30 June 2021; Received in revised form 20 September 2021; Accepted 22 October 2021
Available online 26 October 2021

and establish antibiotic resistant biofilms [8]. More recently, the utilization of silicones for catheter construction and the design of antimicrobial coatings appeared as effective preventative measures against CAUTIs [9]. However, the non-specific protein adsorption on silicone catheters and the formation of a "conditioning layer", where the pathogens easily adhere and form biofilm, limited their utilization for longer periods [10]. Catheters, coated with broad-spectrum antibacterial agents such as antibiotics, metals and metal nanoparticles (NPs) [11,12] have shown variable efficiency in preventing biofilms by either killing the pathogens or inhibiting bacterial growth on the surface of the device. Despite the promising results, the fast and uncontrolled release of the biocides is frequently associated with side effects such as cytotoxicity, hypersensibility, inflammation or development of drug resistance in addition to the low durability of the antimicrobial and antibiofilm effects [13,7]. More innovative approaches for inhibition of bacterial biofilms use enzymes [14,15], antifouling polymers [16] or bactericides with non-specific antibacterial mechanisms (*e.g.* membrane damage and reactive oxygen species generation), which are unlikely to develop resistance [17]. We have successfully explored the antibiofilm enzymes acylase and amylase to engineer stable and efficient multilayer coatings on medical devices [14,15]. These enzymes do not kill bacteria, but interfere with bacterial capacity to coordinate and produce the protective EPM adhesive, thereby inhibiting the biofilm growth and decreasing the risk of resistance development [17].

In this study, for the first time, a durable hybrid nano-coating of antibiofilm enzyme amylase and antibacterial ZnO NPs has been developed onto silicone urinary catheters in a one-step sonochemical process without the need for pre-activation of the silicone material. The hydrolytic enzyme α-amylase has been assembled with antibacterial ZnO NPs templates and simultaneously deposited onto silicone Foley catheters under high-intensity ultrasonic field. The undesirable phenomenon of non-specific protein adsorption on silicones [18] has been transformed into an advantage to improve the stability of the ZnO NPs coating using the enzyme protein as an adhesive that additionally provides biofilm degrading activity. On the other hand, the assembling of amylase with the ZnO nano-templates would ensure the stability of the enzyme upon sonication preventing from protein unfolding and denaturation. Sonochemistry is a versatile and environmentally friendly water-based technique used in our group for production of inorganic (*e.g.* metal oxide), organic (*e.g.* antibiotic) and biological NPs and their simultaneous deposition on a wide range of surfaces [11,19–21].

The hybridization of bioactive proteins with antimicrobial metal oxide nano-templates is an innovative approach that allows to benefit from both the antibiofilm activity of amylase and the bactericidal properties of the inorganic NPs. Herein, the sonochemical nano-formulation of dual active ZnO@AM NPs was expected to synergistically improve the antibiofilm activity of the hybrid nano-coating at minimal, non-toxic levels of the metal oxide biocide. The antimicrobial efficacy of the engineered hybrid nano-coatings has been assessed first *in vitro* under dynamic conditions simulating the urine circulation during catheterization for up to 7 days - the time frame for catheter colonization by pathogens and occurrence of CAUTIs. The incidence of bacteriuria increases daily 3–6% per day after the catheter placement [1]. Moreover, it has been estimated that for each day the catheter is in place, the risk for acquisition of infection in any part of the urinary system (including urethra, bladder, ureters, and kidney) was 10% higher [22]. The biocompatibility of the coatings has been further evaluated upon exposure to mammalian cell lines for the same time period. In addition to the *in vitro* evaluation, the antibiofilm efficacy of the novel coatings for reducing the occurrence of early CAUTIs and possible side effects, such as toxicity and inflammation, has been validated *in vivo* in a rabbit model.

2. Materials and methods

2.1. Materials

ZnO NPs (size <100 nm, zeta-potential = +17.1 ± 0.8 mV) and α-amylase from *Bacillus amyloliquefaciens* (32 mg mL^{-1} protein content and 20 U mg^{-1} specific activity) were purchased from Sigma-Aldrich (Spain). Bacterial species Gram-positive *Staphylococcus aureus* (*S. aureus*, ATCC 25923) and Gram- negative *Escherichia coli* (*E. coli*, ATCC 25922), and human fibroblast (ATCC-CRL-4001, BJ-5ta) and keratinocyte (HaCaT cell line) cells were obtained from the American Type Culture Collection (ATCC LGC Standards, Spain). AlamarBlue Cell Viability Reagent and Live/Dead BacLight kit (Molecular probes L7012) were purchased from Invitrogen, Life Technologies Corporation (Spain). Live/Dead® Kits for mammalian cells viability kit was obtained from Thermo Fischer Scientific (Spain). Polydimethyl/vinylmethyl siloxane urinary (Foley) catheters were provided by Degania Silcone Ltd. (Israel). All other chemicals were purchased from Sigma-Aldrich (Spain) and used without further purification.

2.2. Ultrasound-assisted coating of catheters with ZnO NPs and amylase

The sonochemical coating was performed using an ultrasonic transducer Ti-horn (20 kHz, Sonics and Materials VC750, USA). At first, silicone Foley (size 16 French) catheters were immersed in the ultrasonic pot containing 400 mL aqueous solutions of ZnO NPs (1 mg mL^{-1}) and/or 3.4% amylase (*v*/v) and the coating of the samples was carried out during 15 min at 20 °C and amplitude of 50%. The ultrasonic horn was dipped 2 cm in the solution at a distance from the catheter of approximately 5 cm. After the coating process, the samples were thoroughly washed with distilled water and air-dried. For the *in vivo* studies, entire silicone Foley catheters (size 8 French) were sonochemically coated following the same conditions as described before.

2.3. Surface characterization of the coated catheters

The surface morphology of the functionalized silicone catheters was studies by HRSEM (Quanta 200 FEG from FEI (USA)). Size histogram of the deposited ZnO@AM NPs on the catheter was build using ImageJ software. The amount of the zinc oxide in the coatings was determined after extraction with 0.5 M nitric acid by Inductively coupled plasma (ICP)-atomic emission spectroscopy on an ICP-spectrometer ULTIMA JY2501 (France).

2.4. Stability of the coatings

The durability of the functionalized silicone samples were further evaluated using previously described procedure [14]. Briefly, the silicone material (1 cm) was incubated in artificial urine for 7 days at 37 °C with 20 rpm shaking. The stability of the metal/enzyme coatings was further studied through the changes of the amylase activity in the coatings before and after incubation in artificial urine. ICP technique was used to determine the zinc oxide leaching from the catheter surfaces.

2.4.1. Amylase activity in the coatings

The enzyme activity in the coatings was determined using the 3,5-dinitrosalicylic acid (DNS) assay as previously described [23]. 1 cm of coated catheter was incubated with 2 mL of 1% starch (*w*/*v*) solution in 20 mM sodium phosphate buffer (pH 6.9) for 1 h, at 37 °C with 142 rpm shaking. Then, 1 mL of the sample was incubated with 1 mL DNS reagent for 15 min at 100 °C and the absorbance was measured at 540 nm.

2.5. Quantification of the total biofilm formation

Biofilm formation on the modified silicone materials was assessed

with Gram-negative *E. coli* and Gram-positive *S. aureus* as previously described [14]. Briefly, 1 cm of catheter samples were placed with 1.5 mL of bacteria in tryptic soy broth (TSB, $OD_{600} = 0.01$), and left under static conditions to allow bacteria to form biofilms on the catheters. After 24 h of incubation the total biofilm mass was assessed using crystal violet assay. The same procedure was used to assess the durability of the antibiofilm activity of the coatings after their incubation in artificial urine for 7 days.

2.6. Antibacterial activity

The antibacterial activity of the modified silicone materials was assessed against *E. coli* and *S. aureus*. Briefly, 1 cm of catheter and 2 mL of bacteria in 100 mM phosphate buffered saline (PBS) (CFU $mL^{-1} \approx 10^5$) were placed in 15 mL sterile falcons. The falcons were then incubated for 24 h at 37 °C with 230 rpm shaking. After the incubation, the survived bacteria were plated on selective agars, the plates were incubated for 24 h at 37 °C, and the survived bacteria were count using drop count method.

2.7. Dynamic biofilm inhibition tests

The biofilm activity of the hybrid coating of ZnO@AM NPs was analyzed under dynamic conditions using an *in vitro* physical model of catheterized human bladder as previously described [15]. Briefly, the bladder model was autoclaved (121 °C for 15 min), subsequently the non-treated and coated silicone Foley catheters were inserted into the system and the catheter's balloon was inflated with 5 mL sterile PBS. According to UNE EN1616 (Sterile Urethral Catheters for Single Use), the bladder was filled up to the catheter's eye with sterile artificial urine, pH 6.8 (supplemented with 1 mg mL^{-1} TSB), containing Gram-negative *E. coli* or Gram-positive *S. aureus* (final $OD_{600} = 0.01$ for each bacterium). During the 7 days of catheterization, the model was supplied with sterile artificial urine at a flow rate of 1 mL min^{-1} and maintained at 37 °C. Then, the catheter was removed, and the biofilm formation on the catheter's surface (catheter's tip and balloon) was evaluated. Non-treated silicone Foley catheter served as a control sample (no biofilm inhibition). The evaluation of live and dead bacteria into the biofilms, formed on the catheters were also assessed using Live/Dead BacLight kit assay. Briefly, the silicone samples were stained with a mixture of Syto 9 and propidium iodide (1:1) for 15 min. The biofilms were rinsed with 100 μL of 100 mM PBS and analyzed by fluorescent microscope. The live cells were stained in green and the dead ones in red.

2.8. Cytotoxicity

The cytotoxicity of the coated catheters was evaluated using human fibroblast cells line BJ-5ta and HaCaT keratinocytes. The functionalized catheters were placed in contact with the previously cultured cells and the viable cells were quantified using AlamarBlue assay kit (AlamarBlue®, Invitrogen) after 24 h and 7 days of contact [24]. The cells' morphology was also observed by Live/Dead® Viability/Cytotoxicity assay kit for mammalian cells after exposure of the cells to the coated catheters for 24 h and 7 days as previously described [25].

2.9. In vivo tests in rabbit model

The antibacterial efficacy of the hybrid NPs coatings of amylase and ZnO was assessed *in vivo*. All the experiments were carried out in animal research facility in the Institute of Experimental Morphology, Pathology and Anthropology with Museum, Bulgarian Academy of Sciences (Permit number: 11 30,127) in accordance with the national regulation № 20/01.11.2012 regarding laboratory animals and animal welfare, European legislation, International Standard ISO 10993-1:2009 for biological evaluation of medical devices and were also confirmed by the Institutional Animal Care and Use Committee. New Zealand male rabbits ($n = 9$), 4–5 months of age and mean body weight of 3 kg, were divided into 3 groups as follow: 1st group – is the control group of non-catheterized animals; 2nd group – is the group of animals catheterized with pristine silicone Foley catheters (size 8 French) for 7 days and the 3rd group – is composed of rabbits catheterized with hybrid ZnO@AM NPs-coated catheters for 7 days.

At the beginning of the experiment, all animals were checked clinically for their health status and were diagnosed as healthy. The catheterization procedure was performed under general anesthesia using anesthesia mixture of tiletamine/zolazepam, xylazine and butorphanol in doses 5 mg kg^{-1}, 4 mg kg^{-1}, and 0.15 mg kg^{-1}, respectively, intramuscular administration. After application of lubricant, the sterilized under UV non-treated and treated catheters were aseptically inserted in the *orificium urethrae* externum and the lumen of the urethra. The insertion of the catheters was controlled and visualized using ultrasound (Ultrasound "Mindray DP-20 Vet"). After the insertion, the catheter's balloon was inflated with air and the catheters of group 2 and 3 were secured with several dermal sutures in ventral abdominal wall to prevent their removal from the animal. Medical bandages of the pelvic zone and cervical collars were applied on the rabbits for hygienic and safety purposes, without affecting their capability to feed and drink freely. During the experiments, the heart levels, the breath rates and temperature of the animals were monitored. All animals recover smoothly and no mortality during the anesthesia was observed. After the period of catheterization, blood and urine from each animal group were collected for further analyses.

2.9.1. Microbiological tests

The urine samples from all groups were collected aseptically and subjected to microbiological analysis. From the 1st - control group, 10–20 mL urine was collected after single catheterization followed by immediate removal of the device. In the microbiological studies, 0.1 mL of the collected urine were seeded on a differentiation medium (in triplicate). Additionally, the method of calibrated inoculating loops was performed to detect the presence of microorganisms, as previously described [26]. Microbiological tests were also performed for the catheters after their removal from the animals at the end of the experiment. The indwelling urinary catheters were cut and placed on Chromo-Bio®Urine and Mueller Hinton (MH) agar plates as well as in nutrient rich MH broth (MHB, BUL BIO NCSPB - Sofia). The results after incubation under aerobic conditions at 37 °C for 48–96 h were reported. The quantification of microorganisms was performed by determining the arithmetic mean number of developing colonies and calculating the amount of CFU. Microscopic examinations were performed by Pfeifer method with fuchsin staining under immersion with a digital microscope with a camera (B-190TV, Optika, Italy). The isolation and identification of the bacteria and fungi was carried out in accordance with the Bergey International Identifier [27].

2.9.2. Histopathological examination

On the seventh day of post-catheterization, the animals from each group were sacrificed and humanely euthanized for collecting materials for histology and evaluation of the local tissue reactions and inflammation indications. Tissue samples (1 cm^3 in size) from urethra, urinary bladder and kidneys were first fixed in 10% neutral buffered formalin, then dehydrated in ethanol and embedded in paraffin. Tissue sections (3–5 μm thick) were stained in hematoxylin and eosin and examined by light microscope (Leica DM 5000B, Wetzlar, Germany). The sections were scored for the presence of epithelial desquamation or erosions, fibrosis, inflammatory reactions and foreign body responses or other pathological lesions to evaluate the morphological tissue reactions after the catheterization in both cases. Tissue samples from the control rabbits were used for comparison.

2.9.3. Biochemical analyses

Complete blood count and biochemical analysis were performed by

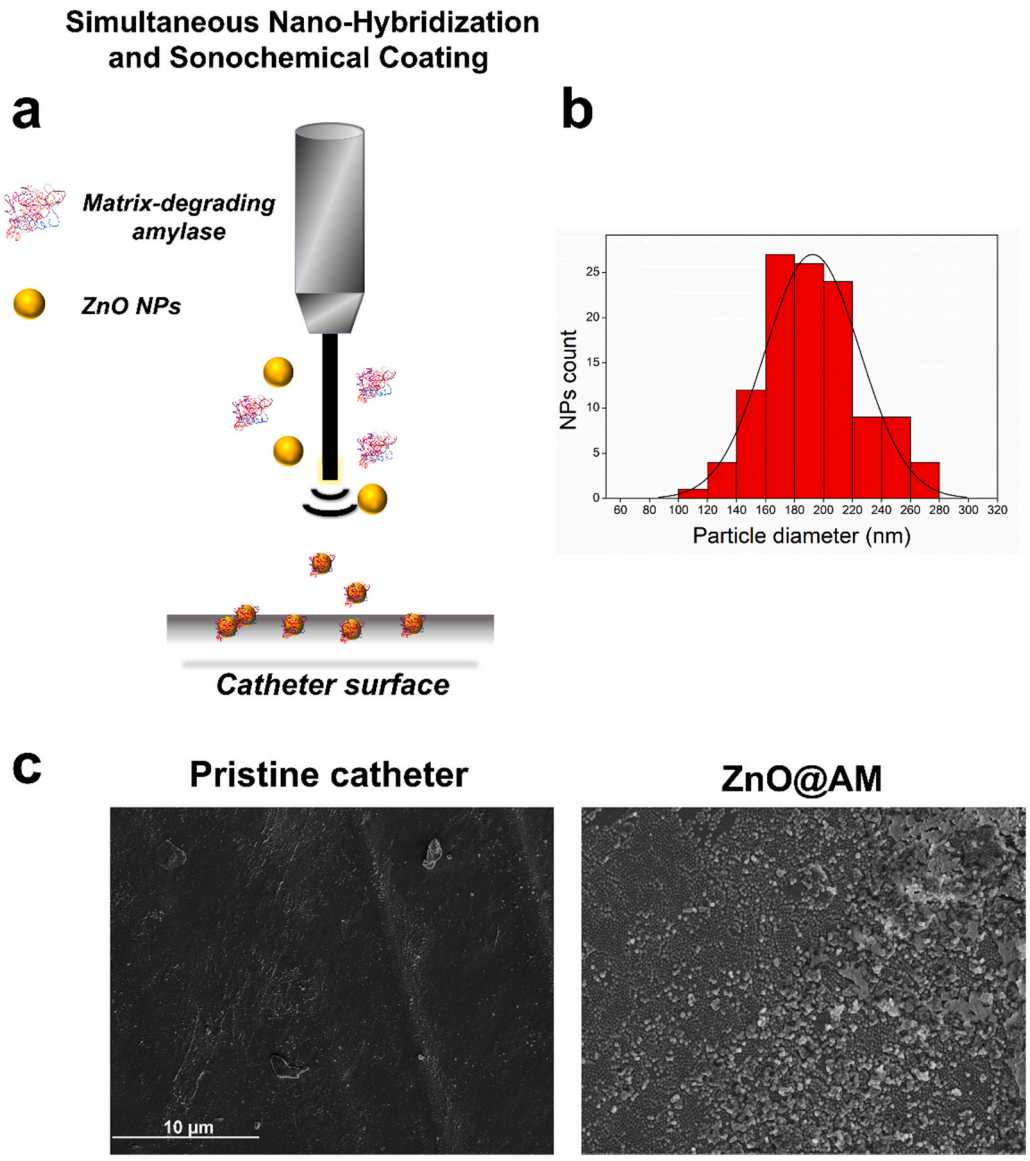

Fig. 1. Surface characterization of sonochemically coated with ZnO@AM NPs silicone catheter. (a) Schematic representation of the US assisted ZnO@AM NPs generation and their deposition on the silicone catheter. (b) Histogram of ZnO@AM NPs size distribution based on the total count of up to 100 NPs using ImageJ software. (c) HRSEM images of pristine and ZnO@AM NPs-coated silicone catheter.

Automatic Hematology Analyzer (Mindray BC - 2800 Vet) and Blood Chemistry Analyzer (MNCHIP Celercare V2). Urine test was carried out using urine analyzer with urine test strips (Urit – 50 Vet). Additionally, whole blood and urine sediment smears were prepared for microscopic examination. Peripheral blood was obtained after puncture of the marginal dorsal vein of the ear and drops were spread on clean sterilized slides and left to air dry. Then, the dried samples were stained with DiaPath May-Grundwald Giemsa Fast Method and were examined by light microscope (Leica DM 5000B, Wetzlar, Germany).

Fresh and mixed sample of each urine was collected in a centrifuge tube and centrifuged using centrifuge (5702R, RH Eppendorf, AG, Germany). After removing of the supernatant, the formed pellet was resuspended in 10 µL urine. The samples, were further processed for microscopic observation.

2.10. Statistical analysis

All data are presented as mean ± standard deviation. For multiple comparisons, statistical analysis by a one-way analysis of variance (ANOVA) followed by post-hoc Tukey test or the unpaired two-tailed Student's *t*-test method, were carried out using Graph Pad Prism Software 5.04 for windows (USA). *P* values less than 0.05 were considered statistically significant.

3. Results and discussions

3.1. Characterization of the coated urinary catheters

High intensity US induced mass transfer, supported by electrostatically-driven self-assembling, was applied to decorate the ZnO NP core with an enzyme shell in order to develop *in situ* dual active bio-nanohybrids. The NPs surface charge in the solution was measured after the coating process. The zeta-potential of the pristine ZnO NPs changed from 17.1 ± 0.8 mV to −22.7 ± 0.5 mV, due to the formation of an amylase layer onto the nano-template. Simultaneously, the obtained hybrid ZnO@AM NPs were deposited onto silicone urinary catheters in a "throwing stone" mode upon the application of US and taking advantage of the non-specific protein adsorption on silicones (Fig. 1a). The surface

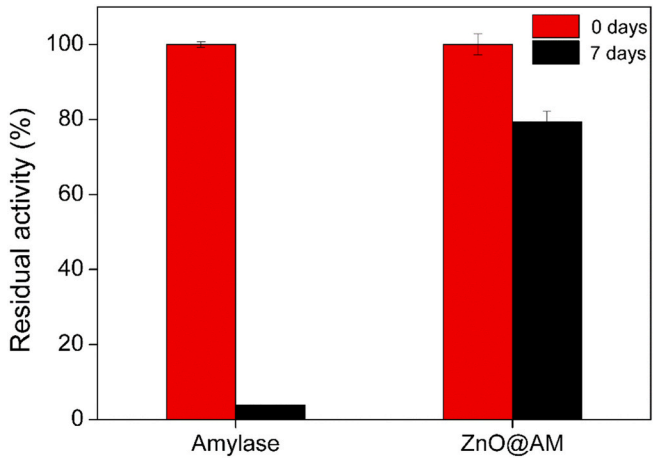

Fig. 2. Enzymatic activity of amylase-containing coating before and after incubation in artificial urine for 7 days with shaking. The results are expressed as the percentage of amylase activity compared to the enzyme before incubation in artificial urine.

morphology of the catheters coated with ZnO@AM NPs was observed using high-resolution scanning electron microscope (HRSEM) (Fig. 1c). The HRSEM analysis of the coated sample showed a dense layer of ZnO@AM NPs with an average size of 192 nm and a narrow NPs size distribution (Fig. 1c).

Previous studies have reported that proteins may adsorb onto colloid particles through a combination of hydrogen bonding, electrostatic, van der Waals, and hydrophobic interactions [28]. In our work, the electrostatic attraction between the positively charged ZnO NPs and negatively charged amylase led to the formation of NP composites that were simultaneously deposited in a uniform layer onto the catheter's surface applying high-intensity US. The formation, growth and collapse of cavitation bubbles, generated upon sonication of liquids, determine the rationale of the deposition process. Microjets and shock waves formed upon the collapse of the acoustic bubbles [12] project the synthesized ZnO@AM NPs at high velocities towards the catheter's surface where the NPs attach by physical interactions between the highly hydrophobic polydimethyl/vinylmethyl siloxane and hydrophobic protein domains. Hydrophobic clusters of a large number of aromatic amino acid residues, *e.g.* tryptophan, tyrosine and phenylalanine, exposed in α-amylase structure promote the protein adsorption [29].

ICP analysis, carried out to determine the amount of ZnO onto the catheters treated with ZnO NPs in presence and absence of amylase, showed up to 10-fold lower amount of ZnO (*ca.* 0.002 wt%) in the hybrid ZnO@AM NPs coating when compared to the coating prepared with only ZnO NPs (*ca.* 0.038 wt%) (Table S1).

3.2. Stability of the coatings in artificial urine

The stability of the coatings in urine is an important parameter to be considered for their practical use. Urine has a complex chemical composition, containing inorganic salts that can affect the catalytic activity of amylase and reduce the antibiofilm potential of the coatings [16,14]. Therefore, the activity of the enzyme on both amylase- and ZnO@AM NPs-coated catheters was assessed after 7 days of incubation in artificial urine (prepared according to DIN EN 1616:1999). The silicone devices coated with amylase alone lost almost 100% of their enzymatic activity after 7 days in contact with urine under continuous agitation. However, the amylase-containing hybrid NPs coating was still active, retaining up to 80% of its initial activity, as confirmed by the production of maltose upon the enzymatic degradation of starch (Fig. 2). α-amylase is a rather robust, industrially relevant enzyme, which activity reflects the changes in the protein conformation under the effect of

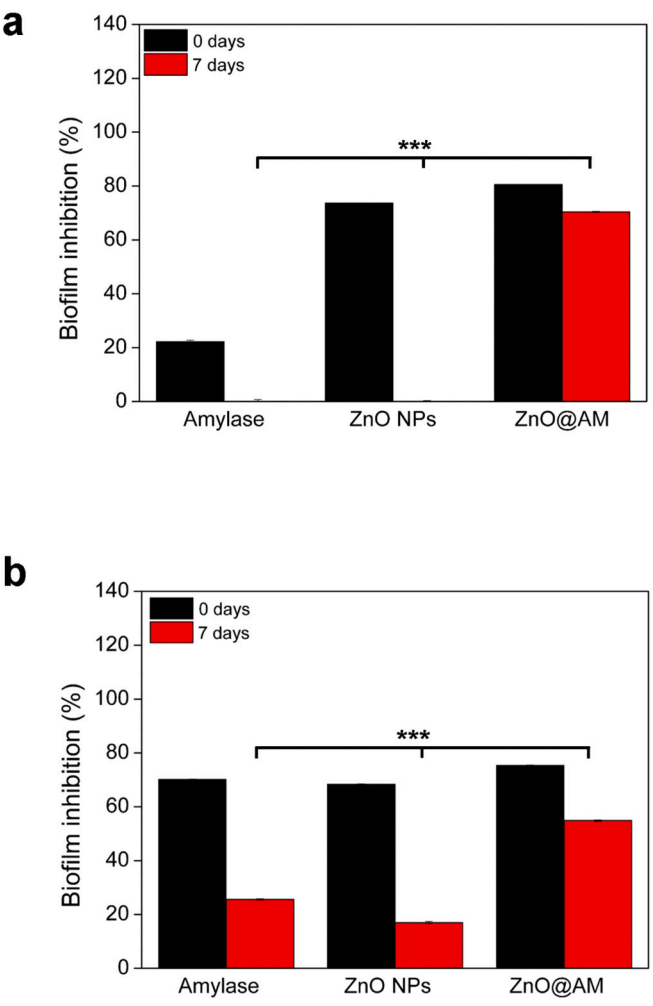

Fig. 3. Biofilm inhibition (%) at static condition of the coated catheters towards (A) *S. aureus* and (B) *E. coli* assessed before and after incubation in artificial urine for 7 days under continuous agitation. The results are represented in %, compared with the biofilm inhibition of pristine catheter (non-inhibition). Stars represent the statistical differences between the different groups of samples; $p < 0.05$.

the application environment. The conformational stability of the enzyme is a function of external variables, such as ionic strength and composition of this environment. Prolonged exposure (7 days) to chemical denaturants, such as urea [29] and salts (NH_4^+ is a strong deactivating cation) in the artificial urine, although not in denaturing concentrations, apparently deactivated the amylase alone, while the assembling of the enzyme onto the metal oxide NP- templates and their subsequent deposition on the catheter ensured the conformational stability of the enzyme protein and its hydrolytic activity in the nano-enabled coating.

Additionally, the leaching of ZnO NPs from the catheters over the same period of incubation in artificial urine was evaluated. ICP measurement quantified the total amount of ZnO in the ZnO and ZnO@AM NPs coatings before and after incubation in artificial urine (Table S1). Considerably lower amount of ZnO was detected on the catheters treated in the presence of amylase in comparison to the catheters treated only with ZnO NPs. On the other hand, the ICP data revealed higher stability of the hybrid ZnO@AM coatings than the individual ZnO NPs materials. High amount (83%) of ZnO initially present on the ZnO@AM NPs-coated catheter remained on its surface after incubation in urine, while only 25% of ZnO was detected in the case of ZnO NPs-coated catheter. The release of ZnO from these coatings is explained with the ZnO NPs

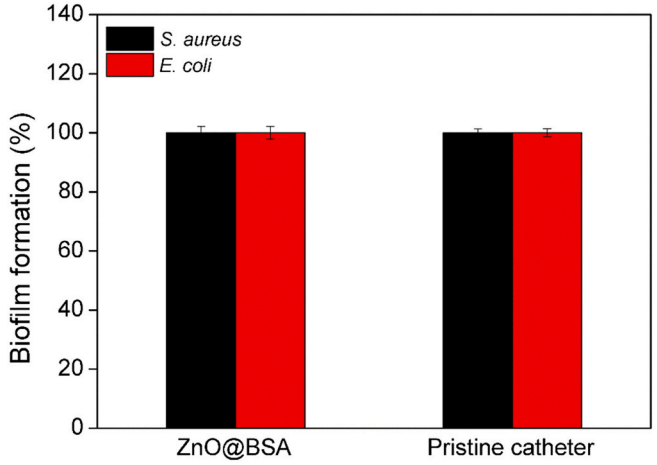

Fig. 4. Biofilm inhibition activity of the ZnO@BSA NPs-coated catheters.

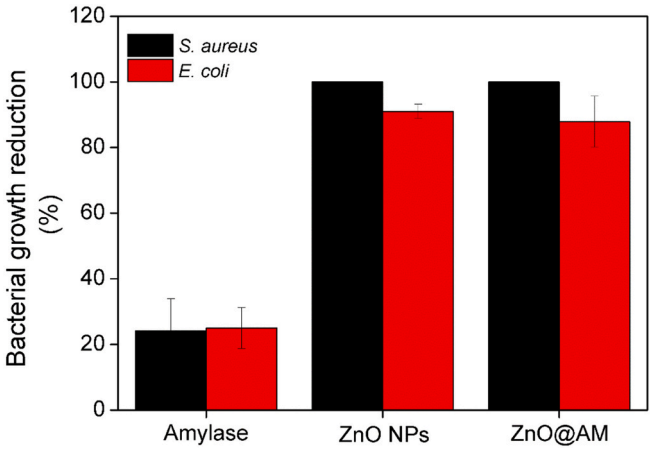

Fig. 5. Antibacterial activity of ZnO NPs and ZnO@AM NPs-coated catheters.

dissolution induced by the phosphates in the artificial urine [30,31]. Apparently, the complexation of ZnO NPs with amylase in the hybrid coatings led to improved stability as confirmed by ICP and HRSEM data. HRSEM images of the coated catheters following their immersion in artificial urine for 7 days (Fig. S1) showed a removal of the ZnO NPs, whereas no significant difference was observed for the hybrid ZnO@AM NPs coating before and after incubation. The sonochemically deposited metal oxides are not stable, and in most cases the substrate requires a pretreatment to improve the coating stability [32,33]. Here, the coating stability was provided by the amylase acting as an adhesive between the hybrid metal oxide/enzyme nanocomplexes and the hydrophobic polydimethyl/vinylmethyl siloxane catheter.

3.3. Antibiofilm activity and functional stability of the coated urinary catheters

The biofilm formation by Gram-positive *S. aureus* and Gram-negative *E. coli*, the most common pathogens found in CAUTIs, was assessed on treated and non-treated catheters under static conditions using crystal violet assay [34]. Catheters, coated either with amylase or ZnO NPs alone inhibited the *S. aureus* biofilm formation by approximately 20% and 70%, respectively (Fig. 3a). In the case of *E. coli*, both amylase and ZnO NPs coatings inhibited the biofilm formation on the catheter by around 70% when compared to non-treated silicone (Fig. 3b). Unlike *E. coli* which produces several types of potential substrates for amylase, *S. aureus* only secretes one dominant EPS involved mainly in the intercellular aggregation of the cells at the surface [35,36]. The amylase-induced degradation of several biofilm adhesives simultaneously is probably the reason for the higher efficacy of amylase-coated catheters on *E. coli* when compare to *S. aureus*.

However, the simultaneous coating with both actives led to inhibition of the total biofilm formation by 81% for *S. aureus* and 75% for *E. coli* (Fig. 3a, b). In the hybrid ZnO@AM NPs the amylase degraded essential for biofilm adhesion and growth polysaccharides [14], inhibiting the biofilm formation by both bacterial strains, and at the same time, increasing the susceptibility of the individual bacterial cells to the bactericidal ZnO NPs at lower concentration. Amylase has been employed in our group both individually and in combination with other enzymes (*e.g.* acylase) [14] or antibacterial agents (*e.g.* silver) [23] to inhibit biofilm maturation, detach pre-formed biofilms, and synergistically increase the susceptibility of the biofilm forming bacteria to biocides. In contrast to commonly used antimicrobials, these hybrid antibacterial/antibiofilm agents eradicate pathogens *via* non-specific mechanisms of action, such as membrane damage, oxidative stress and virulence attenuation, unlikely to induce AMR development [37].

In order to highlight the role of the enzyme and confirm the synergism between ZnO NPs and amylase, sonochemical coatings containing ZnO NPs and non-active protein (bovine serum albumin (BSA)) instead of amylase, were developed. The coatings did not show any ability to reduce the bacterial attachment and biofilm formation (Fig. 4), which demonstrates the relevance of the amylase-assisted EPS degradation for inhibition of the total biofilm formation by the hybrid ZnO@AM NPs coating. Furthermore, catheters coated with amylase did not affect the growth of free-floating bacterial cells, while the ZnO NPs functionalized devices inhibited both *S. aureus* and *E. coli* growth by 100% and 90%, respectively (Fig. 5). These results clearly emphasize the synergy between the amylase and ZnO NPs, which is further reflected in a higher antibiofilm activity at lower concentration of the bactericidal ZnO NPs.

Engineering of stable at use antibiofilm coatings on indwelling urinary catheters is crucial for the effective prevention of CAUTIs. Therefore, the functional stability of the coated catheters, *i.e.* their ability to impair the bacterial attachment and colonization, was assessed after 7 days of incubation in artificial urine under continuous agitation [14]. Catheters functionalized with amylase or ZnO NPs alone, practically lost their ability to inhibit the static biofilm formation of both *S. aureus* and *E. coli* after incubation in urine. However, when amylase and ZnO were simultaneously deposited onto the silicone surface, a negligible decrease of their biofilm inhibition properties was observed in comparison to the non-incubated in urine samples. ZnO@AM NPs coatings lost only 10% and 20% of their antibiofilm activity against *S. aureus* and *E. coli*, respectively (Fig. 3). These results indicate that the hybridization of ZnO NPs and amylase into a nanostructured coating on catheters is an effective antibiofilm approach against both Gram-positive and Gram-negative bacterial strains even after 7 days of exposure to artificial urine.

3.4. Biofilm inhibition tests under dynamic conditions in a model of catheterized human bladder

Despite of the high stability and efficiency of ZnO@AM NPs coatings in controlling the biofilm formation of both Gram-positive and Gram-negative bacteria at static conditions, these conditions do not simulate the real scenario during catheterization. For that reason, the novel hybrid nano-enabled coatings were further challenged in dynamic biofilm inhibition tests in a model of catheterized human bladder (Fig. 6a), where the dynamically varying shear stress associated with urine flow may affect the bacteria adhesion on the surface or provoke coating removal [38]. This model has been widely used in our group for assessing *in vitro* the antibiofilm functionality of catheter coatings [14,16].

Since 80% of bacterial adhesion onto medical devices and the buildup of drug-resistant biofilms occur during the first days after the device insertion [39,40], strategies for prevention of biofilm formation

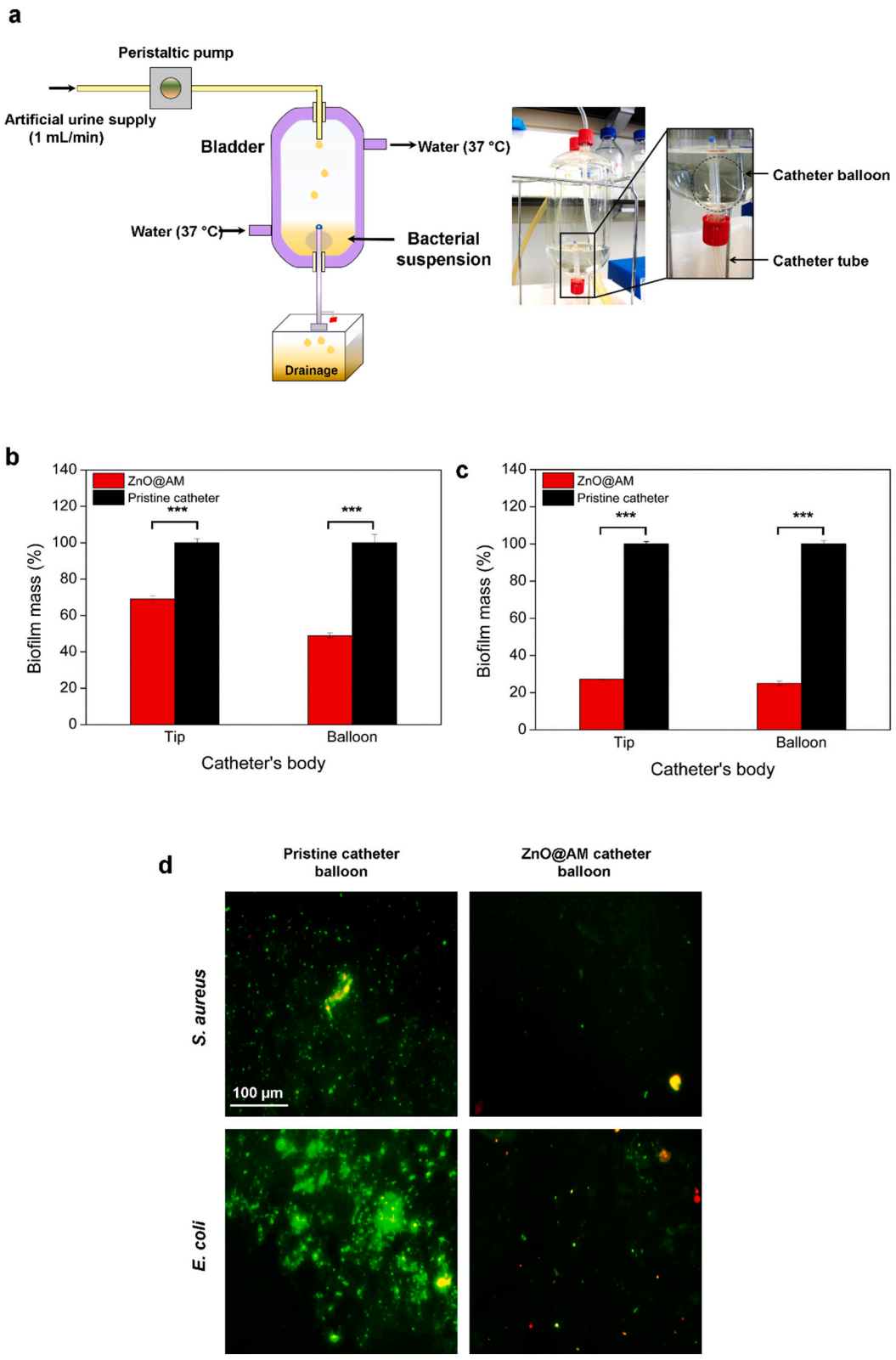

Fig. 6. *In vitro* biofilm inhibition in catheterized bladder model with urine recirculation. (a) *In vitro* model of catheterized human bladder. Total biofilm quantification of (b) *S. aureus* and (c) *E. coli* biofilm mass on ZnO@AM coated urinary catheters. Stars represent the statistical differences between the treated and pristine catheters; $p < 0.05$. (d) Fluorescence microscopy images of live (green) and dead (red) bacteria in the biofilms grown on ZnO@AM-coated and pristine silicone Foley catheter balloon. The green and red fluorescence images are overlaid. (For interpretation of the references to colour in this figure legend, the reader is referred to the web version of this article.)

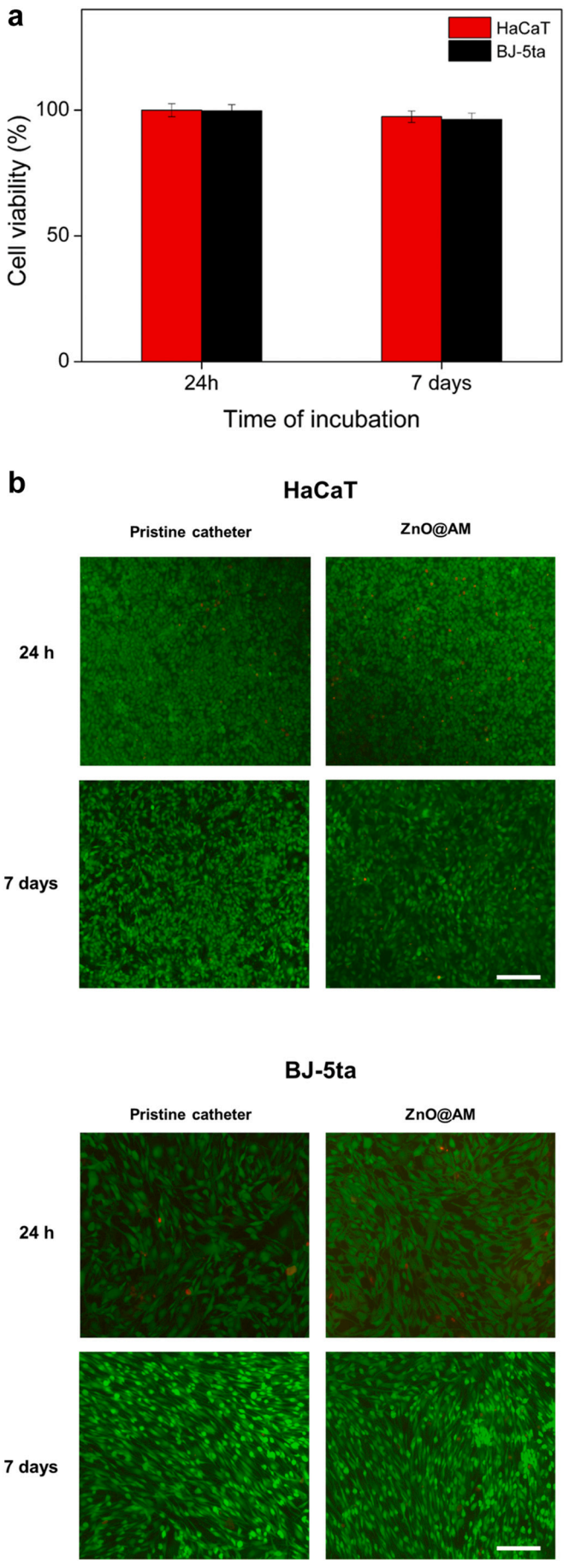

Fig. 7. Viability of HaCaT and BJ-5ta cell lines after exposure to the ZnO@AM NPs- coated catheters assessed by (a) AlamarBlue and (b) Live/Dead kit assays. The green and red fluorescence images are overlaid. Scale bar corresponds to 100 μm. (For interpretation of the references to colour in this figure legend, the reader is referred to the web version of this article.)

within the first days of catheterization are needed. The total biofilm mass formed on the pristine and ZnO@AM NPs-coated Foley urinary devices after 7 days of catheterization was evaluated using crystal violet and Live/Dead kit assays. The sonochemical coating with ZnO@AM NPs led to reduction of both *S. aureus* and *E. coli* total biofilm formation on the catheter's balloon by 60% and 80%, respectively (Fig. 6). The balloon of the catheter inflated inside the bladder is entirely immersed in urine during catheterization. This part of the indwelling urinary device is the most susceptible to colonization and consequent establishment of antibiotic resistant biofilms by urinary tract pathogens. Considering previous works on the biofilm growth in artificial urine [14], we presume that the enzyme in the hybrid coatings affects the *S. aureus* and *E. coli* initial colonization on the catheter surface degrading the polysaccharide adhesives essential for bacterial attachment and growth of biofilms. The degradation of the EPS by amylase inhibits the formation of mature biofilm, further enhancing the bacterial susceptibility to bactericidal ZnO NPs in the coatings. Although, the extent of biofilm reduction was different between the different bacteria the proposed mechanism of antibiofilm action of the hybrid ZnO@AM NPs coatings is valid for both species. The variation in the antibiofilm activity is explained by the different EPS [41] and their functional role in the biofilm establishment as well as different structure of Gram-positive and Gram-negative bacterial membrane [19].

Microscopic observations revealed less *S. aureus* than *E. coli* biofilm formation on the non-treated catheter balloon, explained with the difference between the Gram-positive and Gram-negative bacterial species and their ability to establish *in vitro* biofilms under dynamic conditions [42]. Noteworthy, the biofilm formation by *S. aureus* and *E. coli* on ZnO@AM NPs-coated catheters was completely inhibited and only few individual cells were observed. The appearance of dead bacterial cells (red cells) in the microscopic images was due to the bactericide effect of ZnO NPs. The consistency of the results for the antibiofilm efficiency of ZnO@AM NPs coatings in both static and dynamic conditions clearly demonstrate the potential of these hybrid coatings to prevent the biofilm formation on silicone urinary catheters and therefore decrease the incidence of CAUTIs.

3.5. Cytotoxicity of the coatings

Since ZnO NPs at high concentrations induce cytotoxicity towards mammalian cells [43], the biocompatibility of the developed coatings is an important parameter to be assessed for their clinical application. Cell viability assay was performed to examine the biocompatibility of the coated catheters with two lines of mammalian cells, namely human fibroblast cells and HaCaT keratinocytes. The cells' viability and morphology were observed after 24 h and 7 days of exposure to ZnO@AM NPs-coated catheters (Fig. 7a). The pristine and ZnO@AM NPs-coated catheters did not affect the viability of both fibroblast cells and HaCaT keratinocytes, demonstrating 100% biocompatibility (Fig. 7a). Furthermore, the morphology of the mammalian cells in contact with the catheters was not altered (Fig. 7b), suggesting that the *in vivo* use would not imply any biocompatibility concerns.

3.6. In vivo efficacy assessment of ZnO@AM NPs-coated catheters in a rabbit model

The ability of the coatings to reduce bacterial biofilm growth and respectively the CAUTIs occurrence was assessed *in vivo* in an established rabbit model (Scheme 1). This model does not use specific

(caption on next page)

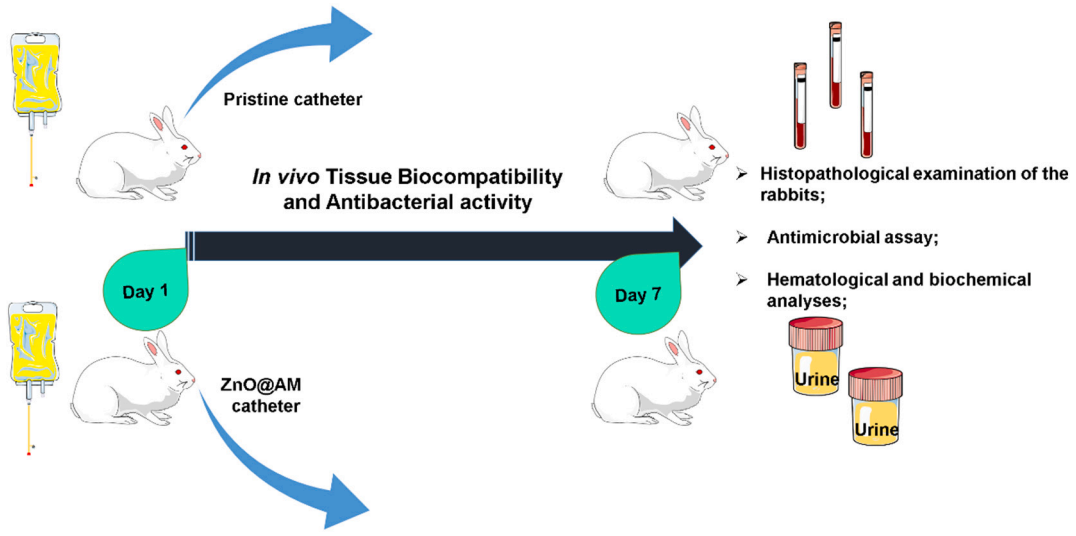

Scheme 1. Schematic representation of the assays performed *in vivo* in a rabbit model.

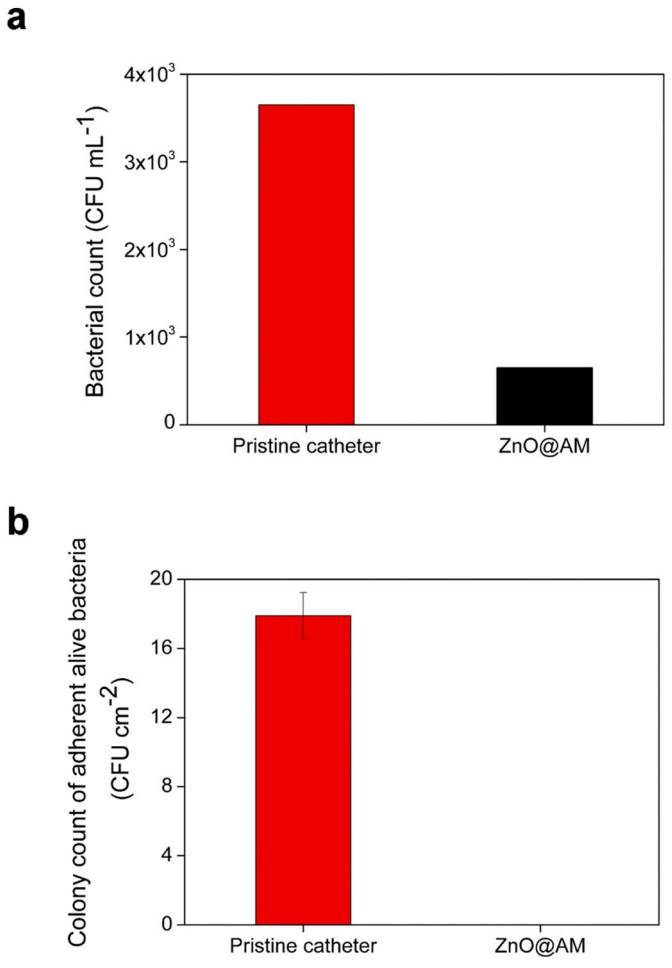

Fig. 8. Antibacterial properties of pristine and ZnO@AM NPs-coated catheters. (a) Colony count of bacteria from the urine samples collected from animals catheterized with pristine and ZnO@AM NPs-coated catheters. (b) Colony count of live bacteria adherent on the non-treated and ZnO@AM NPs functionalized catheters after 7 days of catheterization in the rabbit model.

pathogen inoculum, but rather mimics the natural process by which microorganisms from the surrounding environment colonize the device surface and induce CAUTIs [11]. Additionally, the model allows to assess *in vivo* the biological safety of the coated catheters.

In the *in vivo* tests, animal groups 2 and 3 ($n = 3$), were subjected to catheterization, respectively with pristine and ZnO@AM NPs-coated indwelling urinary catheters, under identical experimental conditions for 7 days (this is the usual time frame for catheter colonization by pathogens and subsequent appearance of CAUTIs). Non-catheterized rabbits (group 1) were used as a control (healthy animals) in all experiments.

3.6.1. *Microbiological analysis of urine and catheters' surfaces for UTIs detection*

At the end of the catheterization period, urine samples and catheters from each group were collected and examined for bacterial contamination. The results from the microbiological studies of the urine collected from group 1 (non-catheterized rabbits) showed that there was no contamination by aerobic and facultative anaerobic microorganisms (data not shown). However, the samples from the urine of the rabbits and the surface of the pristine catheters from group 2 were both colonized with bacteria, mainly from genus *Enterococcus* (Fig. 8). The *Enterococcus* concentration in the urine was $3.65 \times 10^3 \pm 0.54$ CFU ml^{-1} and was sufficient to cause UTI, as confirmed by the appearance of concomitant clinical symptoms such as kidney lesions and signs of developing glomerulonephritis (Fig. 9c) [44]. Bacteria were also detected on the catheter's surface (17.9 ± 1.33 CFU cm^{-2}) and their organization into stable biofilms could further lead to difficult to treat UTIs [45].

In contrast to the animal group catheterized with pristine catheters, the urine samples collected from the animals treated with ZnO@AM NPs-coated catheters (group 3) were practically sterile. Less than 10^3 CFU ml^{-1} (*ca.* $6.5 \times 10^2 + 1.68$ CFU ml^{-1}) bacteria from the genus *Enterococcus* were found in the urine samples, which is not indicative for infection [46]. Although the urine had some bacterial load, the surface of the ZnO@AM NPs-coated catheters remained bacteria-free over the time of catheterization (Fig. 8). These *in vivo* results are in agreement with the *in vitro* observations and confirmed the potential of the hybrid ZnO@AM NPs coating for clinical uses.

3.6.2. *Histopathology after catheterization*

The urethra of the control animals from group 1 did not show any abnormalities (Fig. 7A). Typical features of the epithelial lining, starting

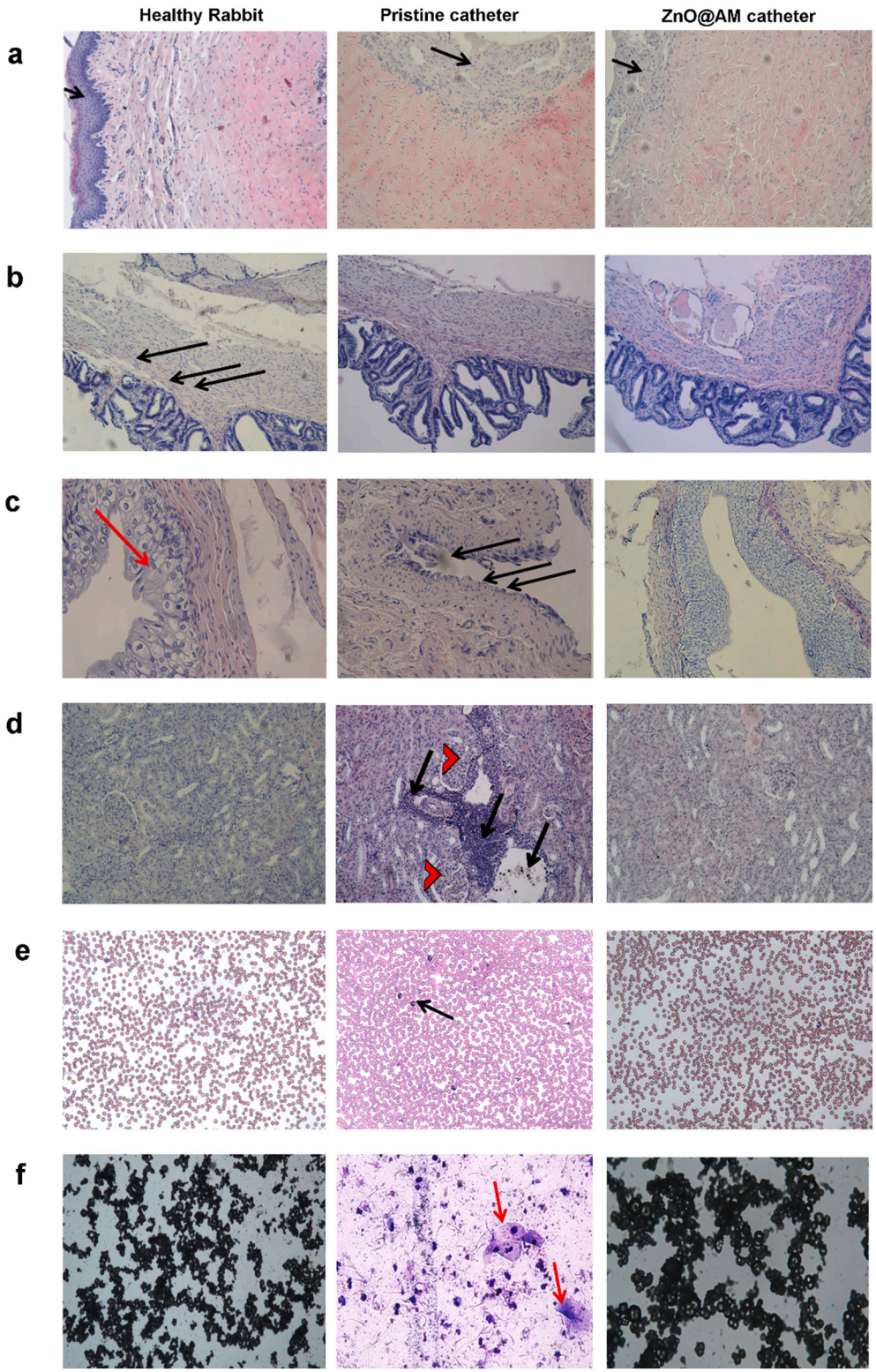

Fig. 9. Histopathology of (a) rabbit penile, (b) prostatic urethra, (c) bladder and (d) rabbit kidney of non-catheterized (group 1) and catheterized with pristine (group 2) and ZnO@AM NPs (group 3) catheters. Black arrows indicate epithelial lining; red arrow displays urinary bladder mucosa with transitional epithelial cell lining; red arrowheads show glomeruli. (e) Blood smears of rabbits. Black arrow indicates the neutrophil granulocytes. (f) Urine sediments of non-catheterized (group 1) and catheterized rabbits (group 2 and 3). Red arrows indicate the umbrella cells from the urinary system mucosal linings. (For interpretation of the references to colour in this figure legend, the reader is referred to the web version of this article.)

with transitional cells near the bladder, followed by pseudostratified, stratified columnar epithelium and stratified squamous approaching the *orificium* (Fig. 9a, black arrow), were observed. In contrast, very mild erosions of the mucosal columnar epithelium, due to the mechanical pressure of the catheters on parts of the penile urethra during catheterization, were detected in the catheterized rabbits from groups 2 and 3 (Fig. 9a, black arrows), while the urothelium in the prostatic urethra was not affected (Fig. 9b). The anatomical position of the penile part of the urethra and the size of the catheters explain these findings.

Significant histopathological alterations due to catheterization were not detected in the bladders of the animals from all groups (Fig. 9c). Groups 1 and 3 had normal morphology of the bladder mucosa with transitional epithelial cell lining (red arrow). Some of the animals in group 2 (non-coated catheters) appeared with mucosal lesion expressed in focal damage of epithelial linings forming microerosions of the cell barrier (Fig. 9c, black arrows) and showed bladder inflammation when

compare to group 3, catheterized with ZnO@AM NPs-coated devices.

The kidneys of the rabbits from group 1 (without catheterization) and group 3 (using ZnO@AM NPs-coated catheter) did not show any pathological lesions (Fig. 9d). Their glomeruli and Bowman's capsules as well as the urinary tubular system were found to be with normal morphology. However, in rabbits from group 2 (pristine catheters) the pathohistological observations showed localized clusters of crescentic glomerulonephritis and vasculitis (extravasation and tissue infiltration from the bloodstream with inflammatory cells) (Fig. 9d, black arrows) and preserved morphology of glomeruli (Fig. 9d, red arrowheads). Zonal infiltration of renal perivascular tissues and circumferential periglomerular renal parenchyma was observed, where the pathology involved abundant local concentration of inflammatory cells. We suggest that this is related to a disorder in the lower urinary tract as the microbiological results revealed bacteria in the urine and on the surface of the pristine catheters.

Morphological observations of all blood smears from non-catheterized rabbits (group 1) and catheterized with ZnO@AM NPs-coated devices (group 3) showed normal cell ratio, unlike the group 2 (pristine catheters), which showed increased number of neutrophil granulocytes (Fig. 9e, black arrow) associated with leukocyturia and indicating the appearance of urothelial infection [47]. In the urine, sediments of the animals from groups 1 and 3 many colorless to yellow-brown calcium carbonate crystals in the form of large or smaller spheroids with radial striations were found (Fig. 9f). Cellular constituents from urothelial linings of bladder, renal pelvis of kidneys or urethra were not seen in these groups. Microscopic aspects of the urine sediments of the animals catheterized with pristine catheters (group 2) revealed leukocytes and erythrocytes, associated with inflammation [48], transitional epithelial cells from the mucosal linings (including umbrella cells) and sperm (Fig. 9f) supporting the pathological processes.

3.6.3. Hematological and biochemical analyses

Hematological and biochemical parameters [49,50] from randomly chosen animals that inform about pathological processes were further analyzed (Table S2 and S3). Generally, the blood counts and biochemistry did not show any serious deviations with the exception of the animals treated with pristine catheters (group 2) developing glomerulonephritis, which white blood cells and monocytes count was higher than the normal levels. The granulocytes count was slightly elevated in rabbits with ZnO@AM NPs-coated catheters, whereas in group 2 the granulocytes increased significantly (Table S2), which is indicative of bacterial infection [51].

Urine samples collected from all animal groups showed slight deviations of some parameters (Table S3). Glucose and ketone values in all studied groups were negative, which means that the rabbits did not present any severe disease. Creatinine was elevated in animals from group 1 and group 2. The histology results from the rabbits treated with the pristine catheter revealed elevated numbers of leukocytes and red blood cells, associated with UTIs. Furthermore, the urine of the animals from this group had pH 6, which is lower compared to pH measured for the healthy non-catheterized animals (group 1) and those treated with ZnO@AM NPs-coated catheters (group 3). Slightly increased levels of blood cells were found in the urine of the catheterized animals (group 2 and 3) due to the movement of the indwelling devices in the bladder lumen causing eventually microtraumas. In a summary, the conducted *in vivo* studies validated: i) the antibiofilm efficiency, ii) capacity to reduce the incidence of CAUTIs, iii) the enhanced life span and iv) safety of the novel ZnO@AM NPs-coated catheters.

4. Conclusions

Silicone urinary catheters were simultaneously coated with matrix-degrading amylase and antibacterial ZnO NPs in a one-step US process. *In vitro*, the engineered nanohybrid coatings demonstrated significant biofilm inhibition against the most common Gram-positive and Gram-negative bacterial representatives found in CAUITs as well as high functional stability upon 7 days of incubation in artificial urine. The ZnO@AM NPs-coated catheters were also able to inhibit the *S. aureus* and *E. coli* biofilm formation by up to 60% and 80%, respectively, under dynamic conditions in an *in vitro* model of catheterized human bladder. The novel antibiofilm coatings were 100% biocompatible with HaCaT and fibroblast cells and subsequently their efficacy was validated *in vivo* in a rabbit model. *In vivo*, the ZnO@AM NPs-coated catheters reduced significantly the growth of *Enterococcus* uropathogens, delaying the early onset of CAUTIs, and at the same time did not induce toxicity to the rabbit's kidney, bladder and urethra after 7 days of catheterization. Overall, the urinary catheters coated with the synergistic combination of biofilm matrix-degrading amylase and antibacterial ZnO NPs appear as a viable solution with high clinical potential for preventing CAUTIs.

CRediT authorship contribution statement

Aleksandra Ivanova, Kristina Ivanova, Tzanko Tzanov, Aharon Gedanken conceived the ideas and designed the experiments; Aleksandra Ivanova and Kristina Ivanova performed functionalization of silicone devices and *in vitro* stability, biofilm inhibition activity, and biocompatibility assays. Ilana Perelshtein performed material morphology characterization by HRSEM and the ICP analysis. Katerina Todorova, Rositsa Milcheva, Petar Dimitrov, and Teodora Popova performed *in vivo* experiments, data collection and analysis. All authors contributed to manuscript preparation and have given approval to the final version of the manuscript.

Declaration of competing interest

The authors declare that they have no known competing financial interests or personal relationships that could have appeared to influence the work reported in this paper.

Acknowledgments

This work was supported by the European project PROTECT “Pre-commercial lines for the production of surface nanostructured antimicrobial and antibiofilm textiles, medical devices, and water treatment membranes” (H2020-720851) and the Spanish Ministry of Economy and Competitiveness (MINECO Project CoatToSafe PID2019-104111RB-100).

Appendix A. Supplementary data

Supplementary data to this article can be found online at https://doi.org/10.1016/j.msec.2021.112518.

References

[1] M.J. Andersen, A.L. Flores-Mireles, Urinary catheter coating modifications: the race against catheter-associated infections, Coatings 10 (2020) 23, https://doi.org/10.3390/coatings10010023.
[2] H. Pinto, M. Simões, A. Borges, Prevalence and impact of biofilms on bloodstream and urinary tract infections: a systematic review and meta-analysis, Antibiotics 10 (2021) 825, https://doi.org/10.3390/antibiotics10070825.
[3] S. Milo, J. Nzakizwanayo, H.J. Hathaway, B.V. Jones, A.T.A. Jenkins, Emerging medical and engineering strategies for the prevention of long-term indwelling catheter blockage, Proc. Inst. Mech. Eng. H 233 (2019) 68–83, https://doi.org/10.1177/0954411918776691.
[4] M. Haque, M. Sartelli, J. Mckimm, M.Abu Bakar, Health care-associated infections-an overview, Infect. Drug Resist. 11 (2018) 2321–2333, https://doi.org/10.2147/IDR.S177247.
[5] Y. Kurmoo, A.L. Hook, D. Harvey, J.F. Dubern, P. Williams, S.P. Morgan, S. Korposh, M.R. Alexander, Real time monitoring of biofilm formation on coated medical devices for the reduction and interception of bacterial infections, Biomater. Sci. 8 (2020) 1464, https://doi.org/10.1039/c9bm00875f.

[6] P. Di Martino, Extracellular polymeric substances, a key element in understanding biofilm phenotype, AIMS Microbiol. 4 (2018) 274–288, https://doi.org/10.3934/microbiol.2018.2.274.

[7] A. Ivanova, K. Ivanova, A. Tied, T. Heinze, T. Tzanov, layer-by-layer coating of aminocellulose and quorum quenching acylase on silver nanoparticles synergistically eradicate bacteria and their biofilms, Adv. Funct. Mater. 30 (2020) 2001284, https://doi.org/10.1002/adfm.202001284.

[8] B.W. Trautner, R.O. Darouiche, Role of biofilm in catheter-associated urinary tract infection, Am. J. Infect. Control 32 (2004) 177–183, https://doi.org/10.1016/j.ajic.2003.08.005.

[9] P. Singha, J. Locklin, H. Handa, A review of the recent advances in antimicrobial coatings for urinary catheters, Acta Biomater. 50 (2017) 20–40, https://doi.org/10.1016/j.actbio.2016.11.070.

[10] K. Ivanova, E. Ramon, J. Hoyo, T. Tzanov, Innovative approaches for controlling clinically relevant biofilms: current trends and future prospects, Curr. Top. Med. Chem. 17 (2017) 1889–1914.

[11] Y. Shalom, I. Perelshtein, N. Perkas, A. Gedanken, E. Banin, Catheters coated with zn-doped CuO nanoparticles delay the onset of catheter-associated urinary tract infections, Nano Res. 10 (2017) 520–533, https://doi.org/10.1007/s12274-016-1310-8.

[12] M. Natan, F. Edin, N. Perkas, G. Yacobi, I. Perelshtein, E. Segal, A. Homsy, E. Laux, H. Keppner, H. Rask-andersen, A. Gedanken, E. Banin, Two are better than one : combining ZnO and MgF 2 nanoparticles reduces Streptococcus pneumoniae and Staphylococcus aureus biofi lm formation on Cochlear implants, Adv. Funct. Mater. 26 (2016) 2473–2481, https://doi.org/10.1002/adfm.201504525.

[13] E. Sánchez-López, D. Gomes, G. Esteruelas, L. Bonilla, A.L. Lopez-Machado, R. Galindo, A. Cano, M. Espina, M. Ettcheto, A. Camins, A.M. Silva, A. Durazzo, A. Santini, M.L. Garcia, E.B. Souto, Metal-based nanoparticles as antimicrobial agents: an overview, Nanomaterials 10 (2020) 1–39, https://doi.org/10.3390/nano10020292.

[14] K. Ivanova, M.M. Fernandes, A. Francesko, E. Mendoza, J. Guezguez, M. Burnet, T. Tzanov, Quorum-quenching and matrix-degrading enzymes in multilayer coatings synergistically prevent bacterial biofilm formation on urinary catheters, ACS Appl. Mater. Interfaces 7 (2015) 27066–27077, https://doi.org/10.1021/acsami.5b09489.

[15] K. Ivanova, M.M. Fernandes, E. Mendoza, T. Tzanov, Enzyme multilayer coatings inhibit Pseudomonas aeruginosa biofilm formation on urinary catheters, Appl. Microbiol. Biotechnol. 99 (2015) 4373–4385, https://doi.org/10.1007/s00253-015-6378-7.

[16] C.D. Blanco, A. Ortner, R. Dimitrov, A. Navarro, E. Mendoza, T. Tzanov, Building an antifouling zwitterionic coating on urinary catheters using an enzymatically triggered bottom-up approach, Appl. Mater. Interfaces 6 (2014) 11385–11393, https://doi.org/10.1021/am501961b.

[17] A. Ivanova, K. Ivanova, T. Tzanov, Inhibition of quorum-sensing: a new paradigm in controlling bacterial virulence and biofilm formation, in: V.C. Kalia (Ed.), Biotechnol. Appl. Quor. Sens. Inhib, Springer Singapore, Singapore, 2018, pp. 3–21, https://doi.org/10.1007/978-981-10-9026-4_1.

[18] H. Zhang, M. Chiao, Anti-fouling coatings of poly(dimethylsiloxane) devices for biological and biomedical applications, J. Med. Biol. Eng. 35 (2015) 143–155, https://doi.org/10.1007/s40846-015-0029-4.

[19] P. Petkova, A. Francesko, I. Perelshtein, A. Gedanken, T. Tzanov, Simultaneous sonochemical-enzymatic coating of medical textiles with antibacterial ZnO nanoparticles, Ultrason. Sonochem. 29 (2016) 244–250, https://doi.org/10.1016/j.ultsonch.2015.09.021.

[20] J. Hoyo, K. Ivanova, E. Guaus, T. Tzanov, Multifunctional ZnO NPs-chitosan-gallic acid hybrid nanocoating to overcome contact lenses associated conditions and discomfort, J. Colloid Interface Sci. 543 (2019) 114–121, https://doi.org/10.1016/j.jcis.2019.02.043.

[21] M. Salat, P. Petkova, J. Hoyo, I. Perelshtein, A. Gedanken, T. Tzanov, Durable antimicrobial cotton textiles coated sonochemically with ZnO nanoparticles embedded in an in-situ enzymatically generated bioadhesive, Carbohydr. Polym. 189 (2018) 198–203, https://doi.org/10.1016/j.carbpol.2018.02.033.

[22] R.J.C. McLean, J.C. Nickel, M.E. Olson, in: H.M. La (Ed.), Biofilm Associated Urinary Tract Infections, Cambridge University Press, Cambridge, UK, 1995, https://doi.org/10.1017/cbo9780511525353.018.

[23] G. Ferreres, A. Bassegoda, J. Hoyo, J. Torrent-burgue, T. Tzanov, Metal – enzyme nanoaggregates eradicate both gram-positive and gram-negative bacteria and their bio fi lms´, ACS Appl. Mater. Interfaces (2018) https://doi.org/10.1021/acsami.8b14949.

[24] A. Ivanova, K. Ivanova, J. Hoyo, T. Heinze, S. Sanchez-Gomez, T. Tzanov, layer-by-layer decorated nanoparticles with tunable antibacterial and antibiofilm properties against both gram-positive and gram-negative bacteria, ACS Appl. Mater. Interfaces 10 (2018) 3314–3323, https://doi.org/10.1021/acsami.7b16508.

[25] K. Ivanova, A. Ivanova, E. Ramon, J. Hoyo, S. Sanchez-Gomez, T. Tzanov, Antibody-enabled antimicrobial nanocapsules for selective elimination of Staphylococcus aureus, ACS Appl. Mater. Interfaces 12 (2020) 35918–35927, https://doi.org/10.1021/acsami.0c09364.

[26] H.L.T. Mobley, M.D. Island, R.P. Hausinger, Molecular biology of microbial ureases, Microbiol. Rev. 59 (1995) 451–480, https://doi.org/10.1128/mmbr.59.3.451-480.1995.

[27] G.M. Garrity, J.A. Bell, T.G. Lilburn, Taxonomic outline of the procaryotes, in: Bergey's Manual of Systematic Bacteriology, 2nd ed., Springer-Verlag, New York, NY, 2004 https://doi.org/10.1007/bergeysoutline200405.

[28] F. Caruso, C. Schüler, Enzyme multilayers on colloid particles: assembly, stability, and enzymatic activity, Langmuir 16 (2000) 9595–9603, https://doi.org/10.1021/la000942h.

[29] K. Singh, M. Shandilya, S. Kundu, A.M. Kayastha, Heat, acid and chemically induced unfolding pathways, conformational stability and structure-function relationship in wheat α-amylase, PLoS One 10 (2015) 1–18, https://doi.org/10.1371/journal.pone.0129203.

[30] C.A. David, J. Galceran, F. Quattrini, J. Puy, C. Rey-Castro, Dissolution and phosphate-induced transformation of ZnO nanoparticles in synthetic saliva probed by AGNES without previous solid-liquid separation. Comparison with UF-ICP-MS, Environ. Sci. Technol. 53 (2019) 3823–3831, https://doi.org/10.1021/acs.est.8b06531.

[31] C. Venkatesh, M. Laurenti, M. Bandeira, E. Lanzagorta, L. Lucherini, V. Cauda, D. M. Devine, Biodegradation and antimicrobial properties of zinc oxide–polymer composite materials for urinary stent applications, Coatings 10 (2020) 1–22, https://doi.org/10.3390/coatings10101002.

[32] P. Petkova, A. Francesko, M.M. Fernandes, E. Mendoza, I. Perelshtein, A. Gedanken, T. Tzanov, Sonochemical coating of textiles with hybrid ZnO/chitosan antimicrobial nanoparticles, ACS Appl. Mater. Interfaces 6 (2014) 1164–1172, https://doi.org/10.1021/am404852d.

[33] U. Shimanovich, I. Perelshtein, A. Cavaco-Paulo, A. Gedanken, Releasing dye encapsulated in proteinaceous microspheres on conductive fabrics by electric current, ACS Appl. Mater. Interfaces 4 (2012) 2926–2930, https://doi.org/10.1021/am3002132.

[34] C. Monteiro, F. Costa, A.M. Pirttilä, M.V. Tejesvi, M.C.L. Martins, Prevention of urinary catheter-associated infections by coating antimicrobial peptides from crowberry endophytes, Sci. Rep. 9 (2019) 1–14, https://doi.org/10.1038/s41598-019-47108-5.

[35] G. Sharma, S. Sharma, P. Sharma, D. Chandola, S. Dang, S. Gupta, R. Gabrani, Escherichia coli biofilm: development and therapeutic strategies, J. Appl. Microbiol. 121 (2016) 309–319, https://doi.org/10.1111/jam.13078.

[36] D.H. Limoli, C.J. Jones, D.J. Wozniak, Bacterial extracellular polysaccharides in biofilm formation and function, Microbiol. Spectr. 3 (2015) 1–30, https://doi.org/10.1128/microbiolspec.mb-0011-2014.

[37] A. Sirelkhatim, S. Mahmud, A. Seeni, N.H.M. Kaus, L.C. Ann, S.K.M. Bakhori, H. Hasan, D. Mohamad, Review on zinc oxide nanoparticles: antibacterial activity and toxicity mechanism, Nano-Micro Lett. 7 (2015) 219–242, https://doi.org/10.1007/s40820-015-0040-x.

[38] N.S. Morris, D.J. Stickler, R.J.C. Mclean, The development of bacterial biofilms on indwelling urethral catheters, World J. Urol. 17 (1999) 345–350, https://doi.org/10.1007/s003450050159.

[39] S.A. Yavari, S.M. Castenmiller, J.A.G. van Strijp, M. Croes, Combating implant infections: shifting focus from bacteria to host, Adv. Mater. 25 (2020) 2002962, https://doi.org/10.1002/adma.202002962.

[40] S. Saint, Clinical and economic consequences of nosocomial catheter-related bacteriuria, Am. J. Infect. Control 28 (2000) 68–75, https://doi.org/10.1016/S0196-6553(00)90015-4.

[41] L. Karygianni, Z. Ren, H. Koo, T. Thurnheer, Biofilm matrixome: extracellular components in structured microbial communities, Trends Microbiol. 28 (2020) 668–681, https://doi.org/10.1016/j.tim.2020.03.016.

[42] S. Stepanović, D. Vuković, P. Ježek, M. Pavlović, M. Švabic-Vlahović, Influence of dynamic conditions on biofilm formation by staphylococci, Eur. J. Clin. Microbiol. Infect. Dis. 20 (2001) 502–504, https://doi.org/10.1007/s100960100534.

[43] L. Fiandra, P. Bonfanti, Y. Piunno, A.P. Nagvenkar, I. Perlesthein, A. Gedanken, M. Saibene, A. Colombo, P. Mantecca, Hazard assessment of polymer-capped CuO and ZnO nanocolloids: a contribution to the safe-by-design implementation of biocidal agents, NanoImpact. 17 (2020), 100195, https://doi.org/10.1016/j.impact.2019.100195.

[44] L. Mody, M. Juthani-Mehta, Urinary tract infections in older women: a clinical review, JAMA, J. Am. Med. Assoc. 311 (2014) 844–854, https://doi.org/10.1001/jama.2014.303.

[45] S. Xiong, X. Liu, W. Deng, Z. Zhou, Y. Li, Y. Tu, L. Chen, G. Wang, B. Fu, Pharmacological interventions for bacterial prostatitis, Front. Pharmacol. 11 (2020) 1–18, https://doi.org/10.3389/fphar.2020.00504.

[46] R. Colodner, T. Eliasberg, B. Chazan, R. Raz, Clinical significance of bacteriuria with low colony counts of enterococcus species, Eur. J. Clin. Microbiol. Infect. Dis. 25 (2006) 238–241, https://doi.org/10.1007/s10096-006-0132-0.

[47] L. Lacerda Mariano, M.A. Ingersoll, The immune response to infection in the bladder, Nat. Rev. Urol. 17 (2020) 439–458, https://doi.org/10.1038/s41585-020-0350-8.

[48] G. Desalegn, O. Pabst, Inflammation triggers immediate rather than progressive changes in monocyte differentiation in the small intestine, Nat. Commun. 10 (2019) 1–14, https://doi.org/10.1038/s41467-019-11148-2.

[49] F.M. Harcourt-Brown, S. Harcourt-Brown, Clinical value of blood glucose measurement in pet rabbits, Vet. Rec. 170 (2012) 674, https://doi.org/10.1136/vr.100321.

[50] A. Melillo, Rabbit clinical pathology, J. Exot. Pet Med. 16 (2007) 135–145, https://doi.org/10.1053/j.jepm.2007.06.002.

[51] S. Döhrmann, J.N. Cole, V. Nizet, Conquering neutrophils, PLoS Pathog. 12 (2016) 1–8, https://doi.org/10.1371/journal.ppat.1005682.